Radioprotection 2013 DOI: 10.1051/radiopro/2013071
Vol. 48, n° 4 , pages 527 à 544

Article

Can the same dose data be estimated from phantoms with different anatomies?

K. KARIMI SHAHRI, L. RAFAT MOTAVALLI*, H. MIRI HAKIMABAD

(Manuscript received 19 August 2012, accepted 29 April 2013)

ABSTRACT **In this paper, the effect of additional adipose and muscle layers was investigated on the effective dose and the organ absorbed dose. Calculations were performed using the Monte Carlo N-Particle Transport Code (MCNP) and the ORNL mathematical phantom for external photon and neutron beams. Variations in adipose and muscle tissue thickness were modeled by adding layers of adipose and soft tissues around the torso of the phantom. The effective dose decreased by about 7%–40% when the thickness of the extra layer increased from 0.5 to 5 cm considering all photon energies (10 keV–10 MeV) and neutron energies (10^{-9}–20 MeV) for anterior-posterior, posterior-anterior, left-lateral, right-lateral, rotation and isotropic irradiation geometries. The results calculated here were compared with those reported in previous studies such as those of the VIPMAN, NORMAN05, MASH-3 and ICRP reference voxel phantoms. Our data shows that adding proper adipose or muscle layers to two very different phantoms can cause similar effective dose values, and also more than half of the organ absorbed doses have satisfactory agreement.**

Keywords: effective dose / organ absorbed dose / addition of adipose layers / conversion coefficients / ORNL modified phantom

1. Introduction

Previous studies have shown that the radiation dose absorbed by organs and tissues determined with a phantom can be applied to a person only if this person has exactly the same anatomical characteristics as the phantom (Johnson *et al.,* 2009; Bolch *et al.,* 2010; Na *et al.,* 2010; Cassola *et al.,* 2011). In recent years, therefore, phantom developers have begun constructing expanded libraries of patient-dependent phantoms using hybrid and mesh models (Lee *et al.,* 2006, 2010; Cassola *et al.,* 2011). In order to further improve the similarity, postural changes were also considered (Sato and Endo, 2008; Cassola *et al.,* 2010a, 2010b). Additionally, statistical phantom construction has been proposed based on statistical organ shape modeling for determination of dose value uncertainties (Babapour *et al.,* 2010; Xu and Liu, 2011). However, producing large libraries of phantoms is time-consuming (Na *et al.,* 2010) and costly as it depends on the use of various software programs (Lee *et al.,* 2008). The effective dose (ED) is the

Physics department, School of Sciences, Ferdowsi University of Mashhad, 91775-1436, Iran.
* e-mail: rafat@ferdowsi.um.ac.ir

protection quantity, the main use of which is the prospective dose assessment for planning and optimization in radiological protection.

The first generation of computational phantoms was based on a stylized model that described the human anatomy via mathematical surface equations (Snyder *et al.,* 1978; Cristy and Eckerman, 1987). In this study, a modified Oak Ridge National Laboratory (ORNL) adult phantom (Miri Hakimabad *et al.,* 2012) that included revisions reported in 1996 (Eckerman *et al.,* 1996) and a thyroid model provided by Ulanovsky (Ulanovsky and Eckerman, 1998) were used. This latter phantom is the revised version of the Medical Internal Radiation Dose (MIRD) phantoms that have been widely used (Lee and Lee, 2006; Lee *et al.,* 2007; Manger *et al.,* 2011).

The aim of this study was to investigate the effects of different anatomies on organ absorbed doses and ED values. Although the ED quantity is based on reference phantoms chosen by convention, this does not mean that one cannot use the ED quantity if other phantoms have been chosen. This study aims to elucidate a way to answer these questions: "can we predict ED values for different anatomies by adding external layers of adipose and muscle tissues to the phantom torso?" and "how much do these extra layers influence organ absorbed doses?" To this end, neutron and photon ED conversion coefficients were calculated for a stylized model (ORNL phantom) (Snyder *et al.,* 1978) under six standard irradiation geometries: anterior-posterior (AP), posterior-anterior (PA), left-lateral (LLAT), right-lateral (RLAT), rotation (ROT) and isotropic (ISO). These data were compared with the results of other phantoms: the VIPMAN (Bozkurt *et al.,* 2000; Chao *et al.,* 2001), the NORMAN05 (Ferrari and Gualdrini, 2007), ICRP reference voxel phantoms (ICRP, 2008, 2010) and the MASH-3 mesh model (Kramer, 2012). Finally, an ORNL adult male phantom was modified by adding layers of adipose and muscle tissues with thicknesses of 0.5 to 5 cm to the surface of the torso to adapt the general anatomy of the ORNL phantom to that of the listed phantoms. Then the dose values were analyzed in this new model.

2. Materials and methods

2.1. Computational models

2.1.1. The modified ORNL stylized model

In the present study, an ORNL phantom was modified by the addition of several layers of adipose and muscle tissues to the torso (Fig. 1). The thickness of the layers was determined on the basis of anatomical differences between the ORNL

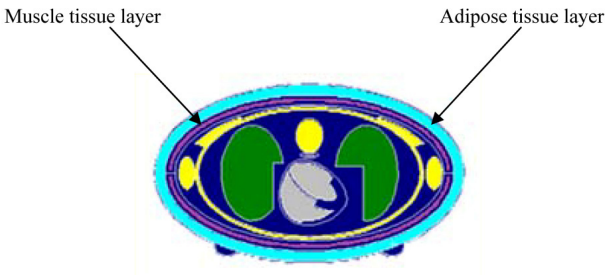

Figure 1 – ***Addition of an adipose and muscle tissue layer to the torso of the ORNL phantom.***

model and other phantoms which were selected for comparison. Different forms were considered for the extra layers (adipose and muscle tissue) for the back of the body, such as adipose layers with thicknesses of 0.5, 0.75 and 1.0–5.0 cm and muscle layers with thickness of 0.5, 0.75, 1.0 and 1.5 cm. In addition, for the front of the body, adipose layers with thicknesses of 1.0–5.0 cm and muscle layers of 0.5–2.0 cm were investigated.

The ORNL torso is a cylinder with an elliptical cross-section. The radius along the major and minor axes of the elliptic section was increased by adding adipose and muscle tissues. First, the muscle layer was placed and then the adipose layer covered it. By appending these layers, the positions of the skin and breasts were altered. Skin was transferred forward by considering the thickness of the external layers added. The front and back skin of the torso was also separated and was simulated by two distinct cells in the Monte Carlo code since the layers added to the front and back of the torso were not the same. Radial changing for breasts was considered. The chemical composition of male breasts was simulated according to the ICRP publication 89 (ICRP, 2002).

The fluence to ED conversion coefficients were calculated using the radiation and tissue weighting factors (w_R and w_T) from the recommendation of ICRP publication 103 (ICRP, 2007).

2.1.2. Voxel models

The second generation of phantoms was voxel models that have been used since the 1980s (Petoussi-Henss *et al.,* 2002; Caon, 2004; Xu *et al.,* 2007). These models are constructed based on computed tomography (CT) or magnetic resonance imaging (MRI) of patients or on high-resolution anatomical photographs of cadavers. Voxel phantoms display better anatomical realism compared with stylized models, but are limited in terms of their ability to alter organ shape,

position and depth, as well as body posture (Lee and Lodwick, 2008). ICRP reference voxel phantoms (Schlattl *et al.,* 2007; ICRP, 2008; Sato *et al.,* 2009) and two other voxel models: the VIPMAN (Bozkurt *et al.,* 2000; Chao *et al.,* 2001) and the NORMAN05 (Ferrari and Gualdrini, 2007) were selected and comparisons were made with these phantoms.

In the case of ICRP reference voxel phantoms, ED conversion coefficients for neutrons and photons were calculated based on ICRP publication 103 (ICRP, 2007) using the PHITS and EGSnrc Monte Carlo codes, respectively (Schlattl *et al.,* 2007; Sato *et al.,* 2009).

ED factors were estimated by using the MCNP and EGS4-VLSI Monte Carlo codes in the VIPMAN model for neutrons and photons, respectively (Bozkurt *et al.,* 2000; Chao *et al.,* 2001). The MCNP Monte Carlo code was used to compute photon ED values in the NORMAN05 model by Ferrari and Gualdrini (2007). In the case of the VIPMAN and NORMAN05 phantoms, published conversion coefficients were evaluated according to ICRP publication 60 (ICRP, 1991; Bozkurt *et al.,* 2000, Chao *et al.,* 2001; Ferrari and Gualdrini 2007). Therefore, ED values on the basis of ICRP publication 103 (ICRP, 2007) were recalculated for these two models using previously calculated organ absorbed doses.

2.1.3. Mesh models

A relatively new and novel computer graphics method has been developed to create the third-generation phantoms using boundary representation (BREP) technologies (Xu, 2010). BREP phantoms appear in the form of non-uniform rational b-splines (NURBS) or polygon mesh surfaces, and are expected to be better suited to geometrical deformation and shape adjustment than voxel phantoms owing to a richer set of computational operations (Zhang *et al.,* 2008a, 2008b; Xu *et al.,* 2008). In this study, data reported from the MASH-3 phantom (male adult mesh in the standing posture) were analyzed (Cassola *et al.,* 2011). Photon ED conversion coefficients for this model were calculated by the EGSnrc Monte Carlo code (Kramer, 2012).

Information on the height and weight of the phantoms mentioned in this study is provided in Table I.

2.2. Dose conversion coefficients

With the MCNP Monte Carlo code, dose conversion coefficients for idealized neutron/photon external exposures were computed as ED per unit neutron fluence/photon air kerma free in air in the entrance plane. The standard irradiation

TABLE I
Information on the phantoms used in this study.

Researcher	Phantom	Total height(cm)	Weight (kg)
Eckerman *et al.* (1996)	ORNL	179	73
ICRP publication 110 (2008)	RMCP	176	73
ICRP publication 110 (2008)	RFCP	163	60
Gualdrini *et al.*	NORMAN05	176	73
Bozkurt *et al.* (2000)	VIPMAN	186	103
Kramer (2012)	MASH-3	176.4	79

geometries investigated were AP, PA, LLAT, RLAT, ROT and ISO in an energy range of 10^{-9}–20 MeV (20 energy points) and 10 keV–10 MeV (23 energy points) for neutron and photon sources, respectively. To simulate a broad parallel photon beam, a disk with suitable radius emitting photons in the surface normal vector direction was defined.

Calculations were performed on a personal computer with the following specifications: Intel(R) Core(TM) i7 CPU 3.07 GHz processor, 6.00 GB of RAM and Windows 7 (64 bits). The evaluated nuclear data came from the ENDF/B-VI cross-section library (Briesmeister, 2000); including the appropriate thermal neutron scattering function S (α, β) for light water at 300 K which was applied to all materials involved in the model (data card: MTm LWTR.07) and photon library. The energy deposited by neutrons and secondary photons in 23 major organs of the phantom was determined using the F6: n, p tally (energy deposition in $MeV.g^{-1}$) in this code. Neutron absorbed doses were calculated assuming that secondary charged particles are absorbed in the interaction region (kerma approximation). Photon simulations were performed in kerma approximation for energies lower than 500 keV and with electron transport for energies above 500 keV. For this reason, the +F6 tally which gives the electron absorbed dose in a cell was employed. The F4 tally, the volume flux tally, for calculation of the red bone marrow absorbed dose for both neutrons and photons was used. In this study, differences are reported as the mean relative difference ± SD for all comparisons.

3. Results

The dose conversion coefficients of large organs could be determined in all geometries by statistical uncertainties of at most around 0.1%. For small organs the statistical uncertainties were around 2% or even less in most cases.

3.1. Comparison with other phantoms' data

The ED conversion coefficients of the ORNL phantom were compared with the values of the ICRP, VIPMAN, NORMAN05 and MASH-3 for neutron and photon sources in AP, PA, LLAT, RLAT, ISO and ROT geometries with the exception of the NORMAN05 and MASH-3, for which the results were compared only for photon beams. Some differences between the results of the ORNL phantom and the other phantoms are shown in Figures 2 to 5. The mean relative differences between the ED results of the ORNL and VIPMAN phantoms are about 8% and 6% for neutrons and photons, respectively (Tabs. II and III) in all geometries with the exception of PA, in which the greatest difference for both photons and neutrons is observable. In this geometry, discrepancies are larger for photon than for neutron beams (23.8 ± 12.3 versus 20.0 ± 12.6). Differences between the NORMAN05 and ORNL data are less than the differences between the ORNL and VIPMAN for photons in all geometries (as shown in Tab. III). Mean relative differences are 5% to 8% for photons in the considered geometries. Comparison between the results of the ORNL and MASH-3 phantoms revealed a great difference in PA geometry. The observed discrepancy was 19.11 ± 37.18, which shows that the mean relative difference and SD are large. The results of the comparison between the ORNL and ICRP models concerning ED values for photons and neutrons are presented in Table V. As the results clearly show, the mean relative differences are below 3% for all irradiation geometries with the exclusion of the LLAT and RLAT for photons, in which relative differences are 6.4 ± 2.0 and 8.0 ± 6.2, respectively. The mean relative differences are below 5% in all irradiation geometries for neutrons. Accordingly, there is a good agreement between these two sets for all geometries.

3.2. Modifications to the ORNL male phantom

The difference in the thickness of the torso adipose and muscle layers in the ORNL phantom and other phantoms is shown in Table VI. The average thickness of the torso adipose and muscle layers in the ORNL phantom is less than selected phantoms. For instance, the back of the ORNL phantom is about 1.5 cm less in thickness than the back of the VIPMAN for both adipose and muscle layers (which makes 3 cm in total). After the differences between the average thicknesses of the ORNL and the other phantoms were specified, extra layers of torso adipose and muscle tissue were added to the front and back of the ORNL phantom to compensate for anatomy differences.

As expected, calculations demonstrated that the thickness of the back layers is important for external exposure to the back (PA) and that the change in the frontal body layers does not affect the ED values for this irradiation geometry. The results

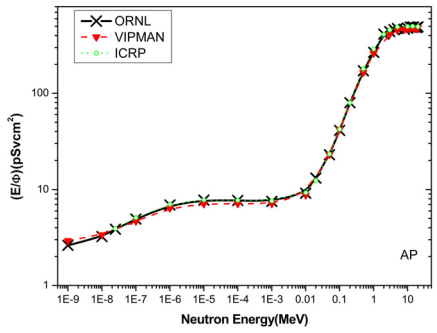

Figure 2 – ***Neutron effective dose conversion coefficients per unit fluence for the whole body in the AP irradiation condition. Comparisons among the ORNL, VIPMAN and ICRP (reference voxel phantoms) were performed.***

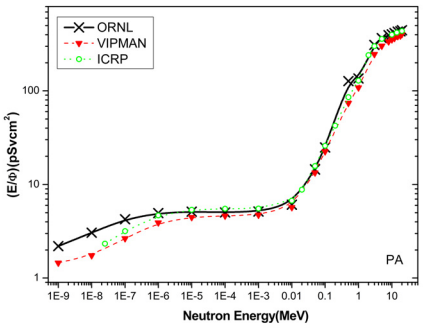

Figure 3 – ***Neutron effective dose conversion coefficients per unit fluence for the whole body in the PA irradiation condition. Comparisons among the ORNL, VIPMAN and ICRP (reference voxel phantoms) were performed.***

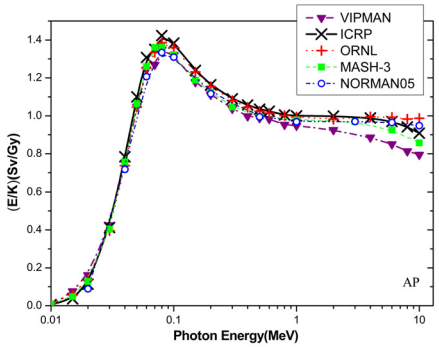

Figure 4 – ***Photon effective dose conversion coefficients per unit air kerma free in air in AP geometry for five phantoms (ORNL, ICRP, VIPMAN, NORMAN05 and MASH-3). The ORNL data differs significantly from the NORMAN05 and MASH-3 results.***

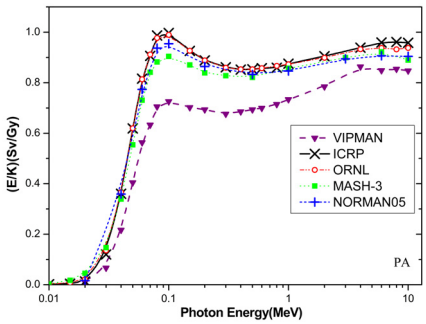

Figure 5 – ***Photon effective dose conversion coefficients per unit air kerma free in air in PA geometry for five phantoms (ORNL, ICRP, VIPMAN, NORMAN05 and MASH-3). The ORNL data differs significantly from the other phantoms' results with the exception of the ICRP data.***

regarding this for neutrons in PA geometry are shown in Figure 6. For AP irradiation, however, only frontal layers are significant. Generally, the ED decreased by 7% to 40% when the thickness of the extra layers increased from 0.5 to 5.0 cm considering all photon and neutron energies and irradiation geometries. The photon conversion coefficients for the different layers of added adipose tissues on the torso with thicknesses of 1.0–5.0 cm for AP geometry are presented in Figure 7.

TABLE II
Comparison of the effective dose and the absorbed dose data in the ORNL before and after adding adipose and muscle layers to the torso (front and back) and the VIPMAN, in all geometries for neutron beams.

Geometry	Relative difference (%)									
	Effective dose		Absorbed dose							
			Liver		Lungs		Stomach		Bladder	
	Before	After	Before	After	Before	After	Before	After	Before	After
AP	4.2 ± 2.9	2.9 ± 3.2	22.4 ± 7.7	17.9 ± 6.1	3.9 ± 3.5	4.6 ± 3.0	26.6 ± 7.6	21.6 ± 5.4	28.1 ± 12.3	21.7 ± 10.6
PA	20.0 ± 12	2.7 ± 1.6	14.4 ± 5.4	8.8 ± 6.1	14.1 ± 8.3	9.7 ± 5.1	9.9 ± 4.2	13.1 ± 8.5	4.1 ± 2.2	19.3 ± 8.2
LLAT	8.1 ± 4.1	2.51 ± 2.4	23.7 ± 9.5	27.7 ± 8.7	24.5 ± 7.4	13.8 ± 4.3	21.4 ± 4.9	13.8 ± 2.4	12.2 ± 8.2	15.1 ± 9.1
RLAT	8.5 ± 4.1	1.7 ± 1.4	26.8 ± 6.3	17.1 ± 5.5	35.8 ± 8.9	27.2 ± 6.8	55.8 ± 21.3	58.9 ± 20.7	17.9 ± 14.4	24.8 ± 11.9
ROT	8.2 ± 3.6	2.4 ± 3.8	14.7 ± 6.0	6.1 ± 3.3	11.0 ± 6.4	3.1 ± 3.1	15.9 ± 6.0	7.7 ± 3.6	15.8 ± 7.4	6.7 ± 5.7
ISO	11.0 ± 5.6	3.9 ± 4.4	14.3 ± 6.1	4.5 ± 3.3	9.2 ± 5.6	1.8 ± 2.4	14.2 ± 6.9	6.0 ± 3.8	15.3 ± 7.6	9.2 ± 4.2

TABLE III
Comparison of the effective dose data in the ORNL before and after adding adipose and muscle layers to the torso (front and back) and the VIPMAN, NORMAN05 and MASH-3 in all geometries for and photon beams.

Model	Geometries	Relative differences (%)	
		Before	After
VIPMAN	AP	4.0 ± 1.9	4.1 ± 5.2
	PA	23.8 ± 12.3	12.1 ± 9.1
	LLAT	8.0 ± 6.2	9.9 ± 3.6
	RLAT	2.4 ± 2.6	8.8 ± 7.1
	ROT	9.1 ± 2.5	4.6 ± 6.5
	ISO	7.5 ± 1.9	2.8 ± 4.4
NORMAN05	AP	7.4 ± 9.9	3.1 ± 4.1
	PA	5.4 ± 7.3	5.00 ± 3.0
	LLAT	7.9 ± 14.5	5.0 ± 2.3
	RLAT	8.2 ± 12.1	4.9 ± 2.1
	ISO	6.2 ± 11.9	5.7 ± 3.0
MASH-3	AP	5.5 ± 9.4	5.5 ± 9.4
	PA	19.1 ± 37.2	7.5 ± 5.6
	ROT	9.0 ± 9.4	5.5 ± 2.4
	ISO	9.8 ± 14.0	6.3 ± 2.33

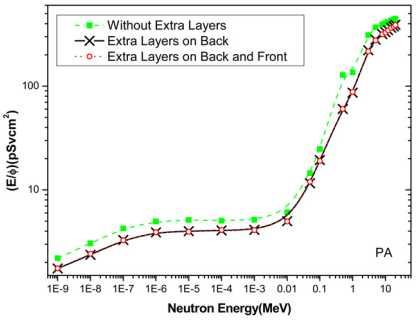

Figure 6 – ***Neutron effective doses per unit fluence for the whole body in the PA irradiation condition. Comparisons between ORNL data before modifications to the model were compared with results after 2.0 cm thickness of adipose and muscle tissues were added to the front and back of the torso or just the back of the ORNL. The results show that frontal layers are not important when radiation exposure enters from the back.***

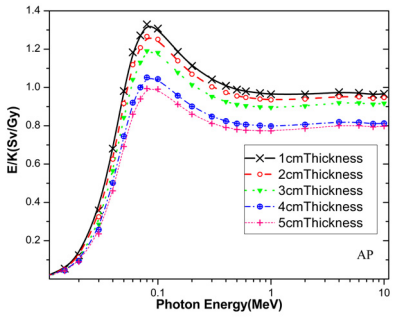

Figure 7 – ***Photon effective dose conversion coefficients per unit air kerma free in air in AP geometry when adipose layers were added to the torso of the ORNL phantom.***

TABLE IV

Comparison of the absorbed dose data in the ORNL before and after adding adipose and muscle layers to the torso (front and back) and the VIPMAN, NORMAN05 and MASH-3 in all geometries for photon beams.

MODEL	Geometry	Relative difference (%)							
		Absorbed dose							
		Liver		Lungs		Stomach		Bladder	
		Before	After	Before	After	Before	After	Before	After
VIPMAN	AP	17.1 ± 10.8	14.3 ± 8.0	14.1 ± 10.4	9.3 ± 4.9	18.5 ± 9.1	15.2 ± 6.4	20.5 ± 15.8	16.8 ± 14.1
	PA	11.2 ± 10.9	5.7 ± 3.5	17.3 ± 14.4	2.8 ± 4.0	9.9 ± 7.5	10.9 ± 13.7	5.1 ± 4.0	25.5 ± 23.8
	LLAT	294 ± 379	345 ± 492	29.5 ± 14.4	23 ± 12.2	51.2 ± 19.9	49 ± 19.5	8.5 ± 12.7	8.2 ± 8.8
	RLAT	59.3 ± 21.2	55.3 ± 22.7	28.9 ± 14.7	21.4 ± 11.6	270.8 ± 258.1	294 ± 334	12.9 ± 15.7	9.3 ± 12.5
	ISO	13.6 ± 9.5	2.8 ± 3.9	16.0 ± 10.8	5.8 ± 5.1	13.2 ± 9.3	4.2 ± 5.6	20.4 ± 15.9	14.4 ± 14.0
	ROT	12.9 ± 8.5	4.0 ± 2.5	18.3 ± 11.5	9.1 ± 5.6	14 ± 7.8	8.6 ± 10.6	17.6 ± 17.5	12.6 ± 14.2
MESH-3	AP	12.6 ± 13.4	12.6 ± 13.4	10.1 ± 7.9	10.1 ± 7.9	2.6 ± 2.4	2.6 ± 2.4	32.9 ± 18.8	32.9 ± 18.8
	PA	32.2 ± 22.2	28.4 ± 20.7	25.7 ± 21.9	21.2 ± 19.9	18.6 ± 16.5	12.7 ± 11.5	23.7 ± 15.2	31.7 ± 21.1
	ISO	19.2 ± 8.1	2.8 ± 4.1	10.9 ± 20.4	5.7 ± 8.4	10.7 ± 12.3	5.8 ± 8.3	23.3 ± 14.5	19.0 ± 13.8
	ROT	2.2 ± 1.3	4.9 ± 6.8	20.5 ± 20	12.2 ± 10.5	2.0 ± 1.0	6.7 ± 7.5	22.6 ± 18.2	17.9 ± 16.6
NORMAN05	AP	1.4 ± 0.6	4.0 ± 4.9	3.6 ± 2.1	1.6 ± 2.0	9.3 ± 5.1	5.8 ± 3.1	1.7 ± 2.4	5.5 ± 6.4
	PA	10.0 ± 9.9	2.6 ± 1.6	13.0 ± 14.8	6.5 ± 7.1	9.0 ± 8.2	14.5 ± 14.0	2.5 ± 3.1	3.5 ± 4.4
	LLAT	92 ± 84.1	102 ± 97	18.2 ± 11.6	14.8 ± 9.8	3.6 ± 5.6	7.7 ± 11.0	4.0 ± 2.60	2.2 ± 2.3
	RLAT	14.3 ± 6.2	9.8 ± 6.2	14.6 ± 8.4	10.7 ± 7.1	46.9 ± 37.8	53.4 ± 44.6	2.9 ± 2.3	7.1 ± 4.1
	ISO	1.7 ± 1.6	7.9 ± 3.1	2.8 ± 1.6	5.2 ± 2.5	1.4 ± 1.2	9.1 ± 4.4	3.8 ± 4.4	9.9 ± 9.1

TABLE V
Comparison of the effective dose and the absorbed dose data between the ORNL and ICRP in all geometries for both neutron and photon beams. A good agreement between results is observed.

Geometry	Relative difference (%)									
	Effective dose		Absorbed dose							
			Liver		Lungs		Stomach		Bladder	
	Photon	Neutron	Photon	Neutron	Photon	Neutron	Photon	Neutron	Photon	Neutron
AP	3.0 ± 2.8	2.9 ± 2.5	8.0 ± 4.1	11.2 ± 5.0	3.4 ± 1.5	8.1 ± 6.5	10.5 ± 19.7	14.3 ± 5	5.7 ± 3.6	9.5 ± 4.1
PA	2.2 ± 3.0	5.36 ± 3.7	9.9 ± 9.6	12.4 ± 4.2	17.9 ± 15.7	12.1 ± 8.7	2.0 ± 1.4	5.3 ± 3.4	18.7 ± 12.6	22.2 ± 10.7
LLAT	6.4 ± 2.0	2.9 ± 2.8	56.1 ± 34.3	39.3 ± 14.8	13.3 ± 8.1	16.1 ± 4.9	20.2 ± 20.5	12 ± 7.7	6.2 ± 8.9	2.3 ± 1.6
RLAT	8.0 ± 6.2	4.90 ± 3.0	7.2 ± 11.4	3.1 ± 3.5	18.2 ± 10.4	24.0 ± 5.8	73.2 ± 52.4	45.9 ± 23.2	11.4 ± 2.6	11.5 ± 5.3
ROT	2.0 ± 1.7	2.2 ± 2.0	8.3 ± 8.3	10.3 ± 4.4	16.3 ± 14.3	4.6 ± 3.8	2.4 ± 1.8	4.9 ± 1.93	2.4 ± 3.1	2.2 ± 2.3
ISO	2.9 ± 1.4	2.4 ± 1.2	2.0 ± 1.1	5.6 ± 2.1	6.4 ± 6.0	3.1 ± 2.3	4.0 ± 4.5	3.4 ± 1.8	2.7 ± 2.5	3.0 ± 2.0

TABLE VI
The difference in thickness of adipose and muscle layers between the ORNL phantom torso and the VIPMAN, MASH-3 and NORMAN05.

Model	Thickness of extra layers (cm)			
	Adipose		Muscle	
	Front	Back	Front	Back
VIPMAN	1	1.5	–	1.5
MASH-3	–	1	–	–
NORMAN05	1	1	–	–

3.3. Effect of extra layers

Detailed comparisons of the ED data in the ORNL before and after adding extra layers with the other phantoms are provided in Tables II, III and V for photon and neutron beams. Accordingly, there is a satisfactory agreement between the ORNL and VIPMAN data after the addition of the above-mentioned thicknesses to the back and front; consequently, the relative differences decrease to 2.0 ± 1.9 and 7.9 ± 4.1 for neutrons and photons, respectively, in PA – a clear agreement is seen for neutrons in this geometry. The only exception in this investigation is RLAT for photons, in which the relative difference increases. In the PA condition, revised EDs conformed to the MASH-3 data with a relative difference of 7.5 ± 5.6 when 1.0 cm thickness of adipose tissue was appended onto the ORNL back. The mean relative differences also decrease to below 6% in other investigated geometries, as depicted in Table III. The similar trend between the ED results of the revised ORNL and NORMAN05 is also observed for photons.

In addition to the ED data, the organ absorbed dose for different tissues was also investigated. Examples of the comparison between the ORNL absorbed dose values, before and after adding extra layers, and the other phantoms are presented in Figures 8a to 8d. Figure 8a depicts the neutron absorbed dose of the adrenals for the VIPMAN in AP, in which the amount of difference decreases to 8.96 ± 6.93 from 57.8 ± 11.41. The considerable reduction in differences in the adrenals is also observed for other geometries. The comparison, in PA, of photon results in the esophagus absorbed dose for the VIPMAN and ORNL phantoms is exhibited in Figure 8b. The relative difference in the ORNL phantom decreases to 12.4 ± 5.6 from 27.33 ± 8.54 when the ORNL anatomy was approximately adapted to that of the VIPMAN. Relative differences in absorbed doses in ORNL phantoms before and after adding extra layers and the listed phantoms for the liver, lungs, stomach and bladder are illustrated in Tables II, IV and V for photon and neutron beams. Generally, modification of the ORNL phantom leads to a decrease in the relative

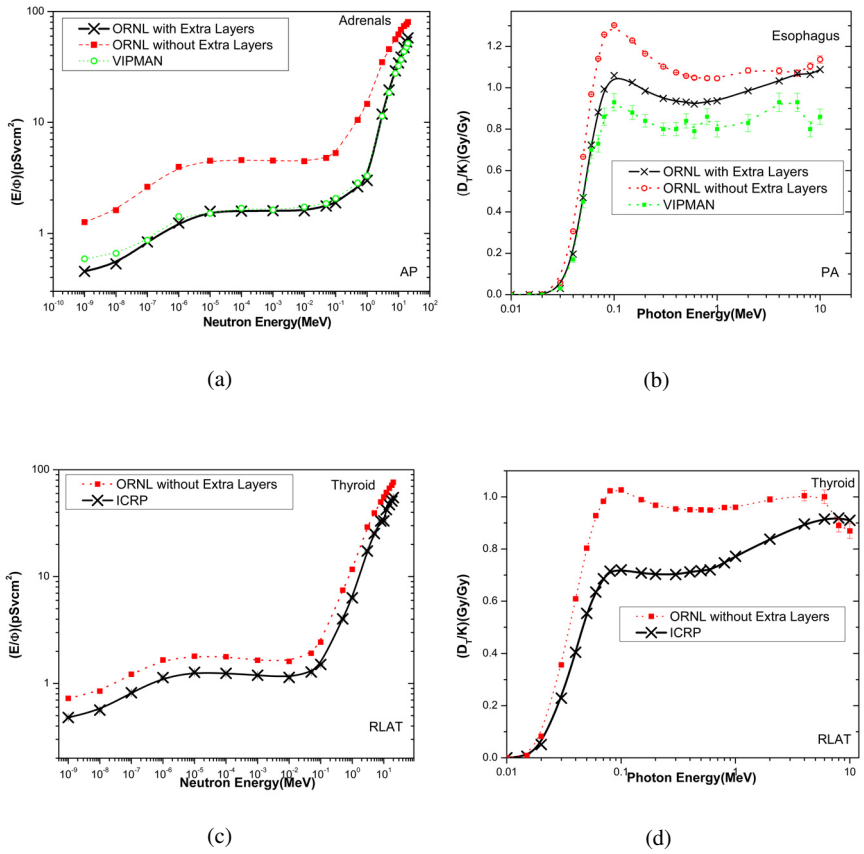

Figure 8 – ***Comparison of conversion coefficients between the ORNL with and without extra layers and the VIPMAN in the adrenals in AP and the esophagus in PA for neutrons (a) and photons (b), respectively. Figures 8c and 8d indicate the neutron and photon absorbed dose for the thyroid in the ICRP male and ORNL phantoms (c and d).***

differences in most organs; however, there are some exceptions. Noticeable decreases can be observed in comparison with the VIPMAN and MASH-3 phantoms for ISO and ROT for both photons and neutrons. Such reduction in relative differences is also seen for the liver and lungs compared with the NORMAN05 phantom in PA. Considerable exceptions to this trend are the liver and stomach in LLAT and RLAT, respectively, for all phantoms. Their relative differences compared with the data from the ORNL phantom before adding extra layers are great, and become larger even after the suitable layers of torso adipose and muscle tissues are appended to the ORNL phantom.

4. Discussion

According to Table V, the ED factors for the ORNL phantom are similar to those of the ICRP but not to the other models studied here. The differences among the anatomies of the different phantoms can be the reason for these data discrepancies, while the role of computational codes may be less important (Sato *et al.,* 2009).

Anatomy differences can be classified into two types: disagreements in organs, shapes and positions, and differences in the general form of the body, especially torso adipose and/or muscle tissues that make up the external shape of the phantom.

In these calculations, external dosimetry was considered. Therefore, external layers of tissue may be preferable over internal organs to study the main reason for ED discrepancies. This was also confirmed when the ORNL phantom was anatomically compared with the ICRP model. It is clear that these models have organs with significantly different shapes (Figs. 8c and 8d). Additionally, differences of approximately 20% are seen between the organ centroids (relative to a point in the center of each phantom). However, about 87% of the EDs of these two phantoms have discrepancies below 5%. These results are reasonable because the ED is the weighted summation of the organ doses and so the influence of anatomical details on it is limited. As previously said, the ED quantity is based on reference phantoms chosen by convention, hence it would be interesting to consider the effect of changing the general anatomy on the organ absorbed dose, which is the quantity of interest for the study of individual dosimetry. Changing the general anatomy includes the extra layers of torso adipose and/or muscle tissues while the anatomical details remain unchanged. How much do these changes affect the relative differences between absorbed doses of different phantoms?

Figures 8a and 8b and also Tables II, IV and V provide a clue to the answer to this question. For instance, organs such as the adrenal glands are more shielded by a thicker layer of muscle and adipose tissue in the VIPMAN voxel phantom than in the ORNL mathematical model. Henceforth, the absorbed doses are smaller in the VIPMAN model than in the ORNL data for all irradiation geometries, especially PA (as shown in Fig. 8b). However, after adding extra layers of adipose and muscle tissues, satisfactory agreement between the adrenal absorbed doses is observed. Detailed investigation of the results of the different organ absorbed doses in the VIPMAN and ICRP phantoms for both photons and neutrons suggest that more than 55% and 65% of them have for the VIPMAN and ICRP phantoms, respectively, in all irradiation geometries, relative differences below 10%, with only 24% of absorbed doses above 25% for both. For all investigated geometries,

the results of the absorbed dose for the NORMAN05 and MASH-3 phantoms also follow a similar trend.

A significant deduction from the above-mentioned discussion is that ED values of the more realistic phantoms (which are very similar to those of real anatomy) are predictable based on the very simple models such as the ORNL phantom. The present data hint that in external dosimetry, the ED is dependent on the distance between organ boundaries and the body surface exposed to the radiation. If all organs or at least the most radiosensitive organs (with w_T) are shielded by the extra layers of adipose and muscle tissue, EDs will decrease. This is further confirmed by Figure 7, which depicts the reduction in the ED values due to the shielding effect of the layers. Withal, more than half of the organ absorbed dose values among different phantoms have an acceptable agreement when the general anatomy of the phantoms is matched approximately to each other. Findings obtained from irradiation of the body by photon and neutron sources in all irradiation geometries support the aforementioned propositions.

The difference between the ORNL and VIPMAN models is about 1.0 cm of adipose tissue in the front of the torso. Besides, the VIPMAN has 1.5 cm adipose and muscle tissue layers in the back in comparison with the ORNL. In all geometries, by annexing these layers to the ORNL phantom, ED results and more than half of the absorbed doses for several organs are similar to those calculated in the VIPMAN phantom (Tabs. II and IV), especially for neutrons. Adding the appropriate amount of adipose or muscle tissue to a simple mathematical phantom such as the ORNL leads to ED results similar to the given phantom, even though their anatomies are quite different. The results of the NORMAN05 and MASH-3 models also confirm these findings for all investigated geometries.

Increasing differences in the photon ED data (in the VIPMAN) for RLAT and those of the absorbed doses in the liver and stomach for LLAT and RLAT in all the listed phantoms are probably related to the external layers of the ORNL sides that are not identical to the other phantoms. The layer of muscle and adipose tissue on the ORNL sides is considered to be thicker than those of other phantoms. The results suggest that the existence of these external layers is more effective for photons than for neutrons when they are appended to the sides.

The agreement between the revised ORNL data and VIPMAN results illustrates that standing height has no significant influence on ED values for studying external beams.

Subcutaneous fat thickness is easily estimated by non-destructive methods such as body apparent resistivity (Murakami and Uchiyama, 2007). Therefore, if

only one phantom is available, we can construct different models by adding extra layers to predict ED values of a large population. Besides, we can closely estimate the absorbed dose data for different organs. This method is simple and efficient, especially for cases in which decisions should be made based on the dosimetric data of a large population such as occupational radiation protection in nuclear power plants or environmental radioactivity.

5. Conclusion

The present study shows the decrease in the organ absorbed doses and the ED values with increasing tissue layers. The results of this study indicate that if only one simple mathematical phantom is available, we can predict ED values for more realistic phantoms by adding external layers of adipose and muscle tissues to the phantom torso.

REFERENCES

Babapour F. *et al.* (2010) Statistical construction of a Japanese male liver phantom for internal radionuclide dosimetry, *Radiat. Protect. Dosim.* **141**, 140-148.

Briesmeister J.F. (Ed.) (2000) MCNP – a general Monte Carlo N-particle transports code: version 4C. Report LA-13709-M, Los Alamos National Laboratory, Los Alamos, 1-427.

Bolch W., Lee C., Wayson M., Johnson P. (2010) Hybrid computational phantoms for medical dose reconstruction, *Radiat. Environ. Biophys.* **49**, 155-68.

Bozkurt A., Chao T.C., Xu X.G. (2000) Fluence to dose conversion coefficients from monoenergetic neutrons below 20 MeV based on the VIP-Man anatomical model, *Phys. Med. Biol.* **45**, 3059-3079.

Caon M. (2004) Voxel-based computational models of real human anatomy: a review, *Radiat. Environ. Biophys*. **42**, 229-235.

Cassola V.F., Lima V.J.D., Kramer R., Khoury H.J. (2010a) FASH and MASH: female and male adult human phantoms based on polygon mesh surfaces: I. Development of the anatomy, *Phys. Med. Biol.* **55**, 133-162.

Cassola V.F., Kramer R., Brayner C., Khoury H.J. (2010b) Posture-specific phantoms representing female and male adults in Monte Carlo-based simulations for radiological protection, *Phys. Med. Biol.* **55**, 4399-4430.

Cassola V.F., Milian F.M., Kramer R., de Oliveira Lira C.A.B., Khoury H.J. (2011) Standing adult human phantoms based on 10th, 50th and 90th mass and height percentiles of male and female Caucasian populations, *Phys. Med. Biol.* **56**, 3749-3772.

Chao T.C., Bozkurt A., Xu X.G. (2001) Conversion coefficients based on the vip-man anatomical model and EGS4-VLSI code for external monoenergetic photons from 10 keV to 10 MeV, *Health Phys.* **81**, 163-183.

Cristy M., Eckerman K.F. (1987) Specific absorbed fractions of energy at various ages from internal photon sources, Oak Ridge, TN: Oak Ridge National Laboratory. ORNL/TM-8381/V1.

Eckerman K.F., Cristy M., Ryman J.C. (1996) The ORNL mathematical phantom series, informal paper, Oak Ridge, TN:Oak Ridge National Laboratory, available at http://homer.hsr.ornl.gov/VLab/mird2.pdf.

Ferrari P., Gualdrini G. (2007) Fluence to organ dose conversion coefficients calculated with the voxel model NORMAN05 and the MCNPX Monte Carlo code for external monoenergetic photons from 20 keV to 100 MeV, *Radiat. Protect. Dosim.* **123**, 295-317.

ICRP Publication 60 (1991) 1990 Recommendations of the International Commission on Radiological Protection, Pergamon, Oxford.

ICRP Publication 89 (2002) Basic Anatomical and Physiological Data for Use in Radiological Protection Reference Values, Pergamon.

ICRP Publication 103 (2007) The 2007 Recommendations of ICRP, Elsevier.

ICRP Publication 110 (2008) Adult Reference Computational Phantoms, Elsevier.

ICRP Publication 116 (2010) Conversion Coefficients for Radiological Protection Quantities for External Radiation Exposures, Elsevier.

Johnson P., Lee C., Johnson K., Siragusa D., Bolch W. (2009) The influence of patient size on dose conversion coefficients: a hybrid phantom study for adult cardiac catheterization, *Phys. Med. Biol.* **54**, 3613-3629.

Kramer R. (2012) External Male standing, http://www.caldose.org/CoeficientesDeConversaoDePeEng.aspx.

Lee C., Lee C., Lodwick D., Bolch W. (2006) A series of 4D pediatric hybrid phantoms developed from the UF series B tomographic phantoms, *Med. Phys.* **33**, 2006-2007.

Lee C., Lee J.K. (2006) Computational anthropomorphic phantoms for radiation protection dosimetry: evolution and prospective, *Nucl. Eng. Technol.* **38**, 239-250.

Lee C., Lee C., Eun Y.H. (2007) Consideration of the ICRP 2006 revised tissue weighting factors on age-dependent values of the effective dose for external photons, *Phys. Med. Biol.* **52**, 41-58.

Lee C. *et al.* (2008) Hybrid computational phantoms of the male and female newborn patient: NURBS-based whole body models, *Med. Phys.* **35**, 2366-2382.

Lee C., Lodwick D. (2008) Hybrid computational phantoms of the 15-year male and female adolescent: Applications to CT organ dosimetry for patients of variable morphometry, *Med. Phys.* **35**, 2366-2382.

Lee C., Lodwick D., Hurtado J., Pafundi D., Bolch W.E. (2010) The UF family of reference hybrid phantoms for computational radiation dosimetry, *Phys. Med. Biol.* **55**, 339-363.

Manger R.P., Bellamy M.B., Eckerman K.F. (2011) Dose conversation coefficients for neutron exposure to the lens of the human eye, *Radiat. Protect. Dosim.* **29**, 1-7.

Murakami K., Uchiyama T. (2007) Bioelectrical Impedance Measurement of Subcutaneous Fat Thickness Using Apparent Resistivity. In: *The 6th International Special Topic Conference on Information Technology Applications in Biomedicine, ITAB 2007*, *November 8-11*, *Tokyo,* pp. 210-212.

Miri Hakimabad H., Rafat Motavalli L., Karimi Shahri K. (2012) Different effective dose conversion coefficients for monoenergetic neutron fluence from 10^{-9} MeV to 20 MeV – A methodological comparative study, *Radioprotection* **47**, 271-284.

Na Y.H., Zhang B., Zhang J., Caracappa P.F., Xu X.G. (2010) Deformable adult human phantoms for radiation protection dosimetry: anthropometric data representing size distributions of adult worker populations and software algorithms, *Phys. Med. Biol.* **55**, 3789-3811.

Petoussi-Henss N., Zankl M., Fill U., Regulla D. (2002) The GSF family of voxel phantoms, *Phys. Med. Biol.* **47**, 89-106.

Sato K., Endo A. (2008) Analysis of effects of posture on organ doses by internal photon emitters using voxel phantoms, *Phys. Med. Biol.* **53**, 4555-4572.

Sato T., Endo A., Zankl M., Petoussi-Henss N., Niita K. (2009) Fluence-to-dose conversion coefficients for neutrons and protons calculated using the PHITS code and ICRP/ICRU adult reference computational phantoms, *Phys. Med. Biol.* **54**, 1997-2014.

Schlattl H., Zankl M., Petoussi-Henss N. (2007) Organ dose conversion coefficients for voxel models of the reference male and female from idealized photon exposures, *Phys. Med. Biol.* **52**, 2123-2145.

Snyder W., Ford M., Warner G., Fisher H.J. (1978) *Estimates of absorbed fractions for monoenergetic photon source uniformly distributed in various organs of a heterogeneous phantom Medical Internal Radiation Dose Committee (MIRD)*, Pamphlet No. 5, revised (New York: The Society of Nuclear Medicine).

Ulanovsky A.V., Eckerman K.F. (1998) Absorbed fractions for electron and photon emissions in the developing thyroid fetus to five years old, *Radiat. Protect. Dosim.* **79**, 419-424.

Xu X.G., Taranenko V., Zhang J., Shi C. (2007) A boundary-representation method for designing whole-body radiation dosimetry models: pregnant females at the ends of three gestational periods-RPI-P3, -P6 and -P9, *Phys. Med. Biol.* **52**, 7023-7044.

Xu X.G., Zhang J.Y., Na Y.H. (2008) Preliminary Data for Mesh-Based Deformable Phantom Development: Is it Possible to Design Person-Specific Phantoms On-demand, In: *The 11th International Conference on Radiation Shielding, ICRS-11, April14-17, 2008, Georgia.*

Xu X.G. (2010) Computational phantoms for radiation dosimetry: a 40-year history of evolution. In: *Handbook of Anatomical Models for Radiation Dosimetry,* (X.G. Xu, K.F. Eckerman, Eds.), chapter 1, pp. 3-41, Taylor and Francis, London.

Xu X.G., Liu T. (2011) Quantifying uncertainty in radiation protection dosimetry using statistical phantoms. In: *The Third International Workshop on Computational Phantoms for Radiation Protection, Imaging and Radiotherapy, August 8-9, 2011, Tsinghua University, Beijing*.

Zhang J.Y., Na Y.H., Xu X.G. (2008a) Size Adjustable Worker Models for Improved Radiation Protection Dosimetry, *Health Phys.* **95**, S50.

Zhang J.Y., Na Y.H., Xu X.G. (2008b) Development of Whole-Body Phantoms Representing an Average Adult Male and Female Using Surface-Geometry Methods, *Med. Phys.* **35**, 2875.